IMU Based Attitude Estimation in the Presence of Narrow-band Noise

Guozheng Lu[1] and Fu Zhang[2]

***Abstract*— In this paper, we consider the attitude estimation based on inertial measurement units (IMUs). We focus on aerial robotic applications where narrow-band vibration noise is present in the IMU measurements due to propeller vibration, aerodynamic turbulence and potential structural modes of the robot platform. The proposed scheme adopts a notch filter to attenuate the narrow-band noise, and incorporates such filter into an indirect extended Kalman filter (EKF) framework to eliminate the induced transient error. Moreover, a least mean square (LMS) method is utilized to estimate the noise dominant frequency in real time, forming an adaptive notch filter that can effectively attenuate narrow-band noise with time-varying dominant frequency. Application to inertially stabilized gimbal systems demonstrates that the proposed method exhibits sufficient noise rejection performance and provides attitude estimation with negligible delay.**

I. Introduction

Attitude estimation, determining the orientation of a rigid body from a series of non-ideal and noisy sensors, is a fundamental task in the robot attitude control, such as unmanned aerial vehicles (UAVs) [1] and multi-axis gimbal system [2]. Attitude are generally measured by two types of sensors: 1) line-of-sight attitude sensors by which vehicle's attitude is obtained via known models and reference, e.g. accelerometers and magnetometers, and 2) integrating the angular velocity of the body frame measured by rate gyros. Accelerometers and gyros (optional magnetometers) are commonly integrated into one package, namely, the inertial measurement units (IMUs), to provide combined measurements of body force, angular rate and orientation. With the advent of micro-electro-mechanical system (MEMS) technology, IMUs can be made very small (e.g. the size of electronic chips) and cheap, being vastly used in consumer electronics (e.g. smart phones, tablets, gaming systems) [3], imaging stabilization devices and micro aerial vehicles (MAVs) [4], etc. However, the MEMS IMU has inherent defects. Accelerometers are stable in a long-term measurement but sensitive to vibrations and translational acceleration, while the fast dynamic gyros randomly drift over time, which, once integrated, results in accumulated errors. Therefore, these two defective features lead to a complementary solution, in which the noise of accelerometers is filtered by gyros while the accumulating errors caused by the gyro drifts are compensated by the long-term accurate measurement of accelerometers.

To achieve precise attitude estimation, various methods have been proposed over decades. A non-linear complementary filter operating on $SO(3)$ was introduced by Mahony *et al* [5]. In this method, the estimation of attitude and gyro bias is corrected by the residual error between the attitude estimation and measurement. This algorithm is with cheap computation and easy implementation. But due to the pre-setting constant correction gains, the estimation is usually suboptimal. Another vastly used attitude estimation approach is the extended Kalman filter (EKF), which is the workhorse of real-time attitude estimation in many robotic applications such as simultaneous localization and mapping (SLAM) [6], visual odometry (VO) [7], visual inertial navigation system (VINS) [8], virtual reality (VR) /augmented reality (AR) [9], etc. EKF is a well known and generic state estimation method for nonlinear systems. It extends the Kalman filter, which was first derived for linear systems and proved to be a minimum variance state estimator, to nonlinear systems by first-order linearization. Schmidt and his collaborators in the Apollo program [10] first applied the EKF framework to attitude estimation based on kinematics model. Nevertheless, in cases of the highly nonlinear dynamics or poor priori estimation of the state, the EKF usually fails [11]. The indirect EKF [12, 13] based on the attitude error state was proposed to diminish the influence of linearization on $SO(3)$ and to avoid the covariance matrix being singular. Furthermore, unscented Kalman filter (UKF) [14] was proved to have relatively superior accuracy, by exploiting the second or higher order of Taylor series expansion of the nonlinear system.

One problem with both standard EKF and UKF based attitude estimation methods is that they assume the observation (attitude measurements, e.g. acceleration, magnetic field, etc.) noise is zero-mean Gaussian white noise, while the measurement noise, however, might be time-varying and non-Gaussian white due to vibrations of structural modes and environmental effects when the vehicle is running. Taking these non-ideal noise into consideration, further studies have been done based on particular assumptions or models. Sebesta *et al* [15] and Sarkka *et al* [16] respectively illustrate methods of adaptively estimating the measurement covariance matrix and tuning the EKF innovation in presence of Gaussian white measurement noise with time-varying covariance. Qian *et al* [17] assumed a multiplicative measurement noise with unknown external disturbances, which lie in a bounded domain. Accordingly, the minimization of the estimated covariance can, to some extent, be achieved by minimizing the upper bound of the estimated covariance. Kumar [18] considered a colored measurement noise. In this scenario, the author first characterized the noise using a second order vibration model and then augmented this model into the standard EKF structure.

[1]Guozheng Lu is with the R&D department, Da-Jiang Innovations Science and Technology Co., Ltd, Shenzhen, China gene.lu@dji.com

[2]Fu Zhang is with the department of Electronic and Computer Engineering, Hong Kong University of Science and Technology, Hong Kong, China eefzhang@ust.hk

Precisely modeling the noise is usually problematic because the noise is susceptible to various time varying factors such as system state and hostile environments. In contrast, digital filters like the low pass filter can effectively attenuate the noise over a wide frequency range, eliminating the need for accurate noise modeling. One drawback of using such filter is that it may introduce considerable delay in attitude estimation, which is one of the main causes of overshoot and even divergence in attitude feedback control. Lozano *et al* [19] and Sanz *et al* [20] proposed to compensate for constant delays by a state predictor, which predicts the current state by delayed state measurement and previous control input. While constant delays can accurately capture delays caused by data transfer or computation, they can barely describe a digital filter (e.g. low pass filter), whose delay is nonlinearly dependent on frequencies of input signals. In this paper, we regard the digital filter as a part of the system model, leading to an augmented attitude kinematics model. We then incorporate such filters into the state observer (e.g. EKF) structure to eliminate the transient error caused by the filter. It is not hard to imagine that when both the state observer predicted output and the actual system output are filtered by the same filter, the resulting estimation error will remain synced and no transient error will present. Accordingly, modeling a digital filter in the observer, instead of approximating to the complex noise, can be a more generic and robust solution.

The original motivation of this paper is to solve the IMU-based attitude estimation problem of multi-axis gimbal systems[2], which have been increasingly used in unmanned aerial vehicles (UAVs) for imaging stabilization. Caused by the aerodynamic turbulence during forward flight and the structural modes of the host aerial vehicle as well as the gimbal system itself, the gimbal system is susceptible various vibrations. These vibrations are translational motions and will be picked up by accelerometers. Since a gimbal system uses the accelerometer measurements to determine its payload attitude, the picked up translational vibrations will behave as a noise and significantly degrade the attitude estimation accuracy. Such a noise, known as vibration noise, is characterized by its narrow bandwidth (e.g. several Hz) and concentration on very low frequency (e.g. under 10 Hz).

In this work, we consider the IMU based attitude estimation in the presence of narrow-band noise. Our main contribution is an attitude estimation algorithm that can effectively attenuate narrow-band noise concentrated at very low frequency range and with time-varying dominant frequency. The developed algorithm comprises three components: an indirect extended Kalman filter framework in discrete time domain, a notch filter that attenuates narrow-band noise concentrated on low frequency range, and a least mean square based adaptive algorithm that accurately identifies the noise dominant frequency in real time. Experiments on actual gimbal systems show that the developed algorithm can accurately track the noise dominant frequency and attenuate the narrow-band noise without inducing much delay in the attitude estimation. Although verified on gimbal systems, the proposed algorithms can be used in other robotic platforms (e.g. UAVs) for attitude estimation in the presence of narrow-band noise.

This paper is organized as follows. Section II briefly introduces the attitude kinematics and the sensors model concerned in this paper. In section III, the standard indirect EKF framework is derived in discrete time domain. Section IV extends the standard EKF to accounts for the dynamics of the notch filter. With additional consideration on noise frequency drifting, adaptive frequency estimation method is adopted in section V. Section VI details the application to an inertially stabilized gimbal system and delivers our experimental results to demonstrate the effectiveness of noise rejection and real-time attitude estimation. Finally, section VI arrives at our conclusion.

II. Attitude Kinematics and Sensor Models

A. Special Orthogonal Group $SO(3)$

Because a gimbal system only involves orientation, it is sufficient to consider the special orthogonal group $SO(3)$, which is the group of all right-handed 3×3 rotation matrix defined as follows

$$SO(3) \triangleq \left\{ \mathbf{R} \in \mathbb{R}^{3\times 3} \,\middle|\, \mathbf{R}^T\mathbf{R} = \mathbf{I}, \det(\mathbf{R}) = 1 \right\} \quad (1)$$

A rotation $\mathbf{R}$ can be interpreted as a rotation about an axis $\boldsymbol{\xi}$ of angle θ. The axis $\boldsymbol{\xi}$ and angle θ are related to the rotation matrix by an *exponential map* [22]:

$$\mathbf{R} \;=\; \exp(\boldsymbol{\theta}_\times) \quad (2)$$

where $\boldsymbol{\theta} = \theta\boldsymbol{\xi}$ and $\|\boldsymbol{\xi}\| = 1$. $\exp(A) = \sum_{n=0}^{\infty} \frac{A^n}{n!}$ is matrix exponential. The subscript operation $\boldsymbol{\theta}_\times$ takes the elements of $\boldsymbol{\theta}$ to form a skew-symmetric matrix as follows

$$\boldsymbol{\theta}_\times \triangleq \begin{bmatrix} 0 & -\boldsymbol{\theta}_3 & \boldsymbol{\theta}_2 \\ \boldsymbol{\theta}_3 & 0 & -\boldsymbol{\theta}_1 \\ -\boldsymbol{\theta}_2 & \boldsymbol{\theta}_1 & 0 \end{bmatrix} \quad (3)$$

The inverse map of $(\cdot)_\times$ is denote as $(\cdot)_\vee$ such that

$$(\boldsymbol{\theta}_\times)_\vee = \boldsymbol{\theta}; \quad \forall \boldsymbol{\theta} \in \mathbb{R}^3 \quad (4)$$

The group of all skew symmetric matrix is called $so(3)$, which is the Lie algebra of $SO(3)$

$$so(3) \triangleq \left\{ S \in \mathbb{R}^{3\times 3} \,\middle|\, S^T = -S \right\} \quad (5)$$

In practice, Eq. (2) is computed by Rodrigue's formula

$$\exp\left(\theta\boldsymbol{\xi}_\times\right) = I + \boldsymbol{\xi}_\times \sin\theta + \boldsymbol{\xi}_\times^2(1 - \cos\theta) \quad (6)$$

The inverse of Eq. (2) is called *logarithmic map*

$$\log \mathbf{R} = \frac{\theta}{2\sin\theta}\left(\mathbf{R} - \mathbf{R}^T\right) \quad (7)$$

where $\theta = \cos^{-1}\left(\frac{tr(\mathbf{R})-1}{2}\right)$. The formula given by (7) is singular at $\theta = \pi$ (or equivalently $tr(\mathbf{R}) = -1$), which should therefore be excluded from $SO(3)$. $\boldsymbol{\theta}_\times = \log \mathbf{R} \in so(3)$ is called the *exponential coordinate* of $\mathbf{R}$.

For $\mathbf{R} \in SO(3)$ and $\boldsymbol{\theta}_\times \in so(3)$, the adjoint map $Ad_{\mathbf{R}}$ is defined as

$$\begin{aligned} Ad_{\mathbf{R}} : so(3) &\mapsto so(3) \\ \boldsymbol{\theta}_\times &\mapsto \mathbf{R}\boldsymbol{\theta}_\times \mathbf{R}^T \end{aligned} \tag{8}$$

If we represent an element on $so(3)$ using its Euclidean coordinate in $\mathbb{R}^3$, the adjoint map can be written as

$$\begin{aligned} Ad_{\mathbf{R}} : \mathbb{R}^3 &\mapsto \mathbb{R}^3 \\ \boldsymbol{\theta} &\mapsto \mathbf{R}\boldsymbol{\theta} \end{aligned} \tag{9}$$

It is straight forward to prove that

$$e^{Ad_{\mathbf{R}}\boldsymbol{\theta}_\times} = \mathbf{R}e^{\boldsymbol{\theta}_\times}\mathbf{R}^T; \forall \mathbf{R} \in SO(3), \boldsymbol{\theta}_\times \in so(3) \tag{10}$$

Observing that a rotation $\mathbf{R}$ satisfies $\mathbf{R}^T\mathbf{R} = \mathbf{I}$, differentiating both side yields $\dot{\mathbf{R}}^T\mathbf{R} + \mathbf{R}^T\dot{\mathbf{R}} = 0$. Let $\boldsymbol{\omega}_\times = \mathbf{R}^T\dot{\mathbf{R}}$, then $\boldsymbol{\omega}$ is the instantaneous body angular velocity [22] and

$$\dot{\mathbf{R}} = \mathbf{R}\boldsymbol{\omega}_\times \tag{11}$$

Note that elements of Lie algebra $so(3)$ can represent a velocity as in (11) or can represent the matrix logarithm (i.e. exponential coordinate) of an instantaneous state as in (7). In addition, if the rotation is about a fixed orientation $\boldsymbol{\omega}$ represented in body frame (intrinsic), (11) implies that

$$\mathbf{R}(t) = \mathbf{R}(0)e^{\boldsymbol{\omega}_\times \theta(t)} \tag{12}$$

where $\theta(t)$ is the total rotation angle from time zero. The proof is made by respectively substitution.

Theorem 2.1: Let $\mathbf{R}(t)$ be a smooth curve on $SO(3)$, $\boldsymbol{\theta}_\times(t) = \log(\mathbf{R}(t)) \in so(3)$ be the exponential coordinate of $\mathbf{R}(t)$, $\boldsymbol{\omega} = \mathbf{R}^T\dot{\mathbf{R}}$ the body velocity, then

$$\boldsymbol{\omega}_\times = \int_0^1 Ad_{e^{-\lambda\boldsymbol{\theta}_\times}} \frac{d\boldsymbol{\theta}_\times}{dt} d\lambda \tag{13}$$

Theorem 2.1 is called the integral formula, the proof of which can be found in [23], where the closed form solution of the integral was also obtained

$$\boldsymbol{\omega} = \mathbf{M}(\boldsymbol{\theta})^T\dot{\boldsymbol{\theta}} \tag{14}$$

where

$$\mathbf{M}(\boldsymbol{\theta}) = I + \left(\frac{1-\cos\|\boldsymbol{\theta}\|}{\|\boldsymbol{\theta}\|}\right)\frac{\boldsymbol{\theta}_\times}{\|\boldsymbol{\theta}\|} + \left(1 - \frac{\sin\|\boldsymbol{\theta}\|}{\|\boldsymbol{\theta}\|}\right)\frac{\boldsymbol{\theta}_\times^2}{\|\boldsymbol{\theta}\|^2} \tag{15}$$

B. Sensor Models

The body frame is practically defined as the frame of the IMU enclosure, where the axis orientation of gyros and accelerometers is assumed to be calibrated and aligned with the IMU enclosure. As a result, the measurement of gyros and accelerometers is immediately interpreted as that in the body frame.

The gyro is typically modeled as [13]

$$\boldsymbol{\omega}_{m_k} = \boldsymbol{\omega}_k + \mathbf{b}_k + \mathbf{n}_{r_k} \tag{16}$$

$$\mathbf{b}_k = \mathbf{b}_{k-1} + \mathbf{n}_{w_{k-1}}\Delta t \tag{17}$$

where Δt is the sampling time, $\boldsymbol{\omega}_{m_k}$ and $\boldsymbol{\omega}_k$ are respectively the measured and true angular velocity at the k-th time step, $\mathbf{n}_r$ is the measurement noise and assumed to be Gaussian white, and $\mathbf{b}$ denotes the random-walk gyro bias driven by another Gaussian white noise $\mathbf{n}_w$. Combining (11), (16) and (17) yields the system state space model in discrete time domain

$$\mathbf{R}_k = \mathbf{R}_{k-1}\exp\left((\boldsymbol{\omega}_{k-1})_\times \Delta t\right) \tag{18a}$$

$$\boldsymbol{\omega}_{k-1} = \boldsymbol{\omega}_{m_{k-1}} - \mathbf{b}_{k-1} - \mathbf{n}_{r_{k-1}}$$

$$\mathbf{b}_k = \mathbf{b}_{k-1} + \mathbf{n}_{w_{k-1}}\Delta t \tag{18b}$$

Considering the vibration noise, the accelerometer noise model is no longer Gaussian white. Instead, the measurement $\mathbf{a}_m$ is related to the gravity $\mathbf{g}$ and translational acceleration $\mathbf{a}_c$, both expressed in body frame, by [25]

$$\mathbf{g}_k = \mathbf{R}_k^T\mathbf{e}_3 \tag{19a}$$

$$\mathbf{a}_{m_k} = -\mathbf{g}_k + \mathbf{a}_{c_k} + \mathbf{d}_k + \mathbf{n}_{a_k} \tag{19b}$$

where $\mathbf{e}_3 = [0\ 0\ 1]^T$, $\mathbf{d}$ denotes the vibration noise and $\mathbf{n}_a$ is Gaussian white noise to capture the random measurement noise. (19) simply states the fact that the accelerometer measures all forces acted on the body but gravity. This agrees with two common facts: 1) a free falling accelerometer leads to zero measurements; and 2) a static accelerometer reads an acceleration that is opposite to gravity. Also note that the translational acceleration $\mathbf{a}_c$ can be compensated via methods like GPS-derived acceleration, thus can be omitted from (19b).

In our concerned application, the yaw angle of the gimbal payload is computed from the host UAV attitude and the forward kinematics [2]. Its measurement model takes the following form, which is essentially the formula for computing yaw angle in ZXY Euler angles from a rotation matrix.

$$\psi_k = -\arctan\frac{\mathbf{e}_1^T\mathbf{R}_k\mathbf{e}_2}{\mathbf{e}_2^T\mathbf{R}_k\mathbf{e}_2} \tag{20a}$$

$$\psi_{m_k} = \psi_k + n_{y_k} \tag{20b}$$

where $\mathbf{e}_1 = [1\ 0\ 0]^T$ and $\mathbf{e}_2 = [0\ 1\ 0]^T$, n_y is the measurement noise caused by host vehicle attitude measurements and gimbal joint measurements. In cases where magnetometer is used, the measurement model will take a similar form as that of accelerometer in (19).

III. Indirect Extended Kalman Filter in Discrete Time Domain

The kinematic model (18) is problematic for the use of extended Kalman filter, due to the orthogonality constraint on the rotation matrix $\mathbf{R}$. This leads to singularity issues when propagating the corresponding covariance matrix [12]. For the sake of numerical stability, we adopt the method in [12], which is known as the error kinematic model that converts the original kinematic model in (18) by its deviation (i.e. the error attitude) from the predicted attitude. The extended Kalman filter (EKF) building on such an error kinematic model is thus called the indirect EKF. The original derivation in [12] was based on continuous time domain

and discretization. In this paper, we re-derived the indirect EKF based on the discrete time domain model (18) and then extend it to handle narrow-band noise.

A. State Propagation of The Primal System

To start with, let us be at present time step k, with the a-posteriori state estimate at previous step $\widehat{\mathbf{R}}_{k-1|k-1}$ and $\widehat{\mathbf{b}}_{k-1|k-1}$. The goal of the EKF is to obtain the a-priori estimate and the a-posteriori estimate at the present time step.

The a-priori estimate can be immediately obtained from the state equation (18) by following the standard extended Kalman filter (EKF), i.e.,

$$\widehat{\mathbf{R}}_{k|k-1} = \widehat{\mathbf{R}}_{k-1|k-1} \exp\left((\widehat{\boldsymbol{\omega}}_{k-1|k-1})_\times \Delta t\right) \tag{21a}$$

$$\widehat{\boldsymbol{\omega}}_{k-1|k-1} = \boldsymbol{\omega}_{m_{k-1}} - \widehat{\mathbf{b}}_{k-1|k-1} \tag{21b}$$

$$\widehat{\mathbf{b}}_{k|k-1} = \widehat{\mathbf{b}}_{k-1|k-1} \tag{21c}$$

B. Propagation of The Error State System

Since the state $\mathbf{R}$ is on a nonlinear differential manifold $SO(3)$, directly applying the EKF on the state $\mathbf{R}$ will cause singularity in the convariace propagation. To avoid this, we transform the primal system into its error state predicted over time steps $\tau \geq k-1$ as below

$$\delta\mathbf{R}_\tau \triangleq \widehat{\mathbf{R}}_{\tau|k-1}^T \mathbf{R}_\tau \tag{22a}$$

$$\Delta\mathbf{b}_\tau \triangleq \mathbf{b}_\tau - \widehat{\mathbf{b}}_{\tau|k-1} \tag{22b}$$

where $\widehat{\mathbf{R}}_{\tau|k-1}$ is the attitude prediction at step τ based on all outputs up to the previous time step $k-1$, and is updated by the following state equation

$$\widehat{\mathbf{R}}_{\tau|k-1} = \widehat{\mathbf{R}}_{\tau-1|k-1} \exp\left((\widehat{\boldsymbol{\omega}}_{\tau-1|k-1})_\times \Delta t\right) \tag{23a}$$

$$\widehat{\boldsymbol{\omega}}_{\tau-1|k-1} = \boldsymbol{\omega}_{m_{\tau-1}} - \widehat{b}_{\tau-1|k-1}$$

$$\widehat{\mathbf{b}}_{\tau|k-1} = \widehat{\mathbf{b}}_{\tau-1|k-1} \tag{23b}$$

for $\tau \geq k$. From the definition in (22), one can easily obtain

$$\delta\widehat{\mathbf{R}}_{k-1|k-1} = \widehat{\mathbf{R}}_{k-1|k-1}^T \widehat{\mathbf{R}}_{k-1|k-1} = \mathbf{I}_{3\times 3} \tag{24a}$$

$$\Delta\mathbf{b}_{k-1|k-1} = \widehat{\mathbf{b}}_{k-1|k-1} - \widehat{\mathbf{b}}_{k-1|k-1} = \mathbf{0}_{3\times 1} \tag{24b}$$

The key idea of indirect EKF is that it estimates the error state (i.e. $\delta\mathbf{R}$ and $\Delta\mathbf{b}$) instead of the original system state (i.e. $\mathbf{R}$ and $\mathbf{b}$). To do so, the state equation of the error state is required. Substituting the state equation of ground truth system (18) and the predicted system (23) into error state system (22) leads to

$$\delta\mathbf{R}_\tau = \exp\left(-(\widehat{\boldsymbol{\omega}}_{\tau-1|k-1})_\times \Delta t\right) \delta\mathbf{R}_{\tau-1} \exp\left((\boldsymbol{\omega}_{\tau-1})_\times \Delta t\right) \tag{25a}$$

$$\Delta\mathbf{b}_\tau = \Delta\mathbf{b}_{\tau-1} + \mathbf{n}_{w_{\tau-1}} \Delta t \tag{25b}$$

Let $\delta\theta$, $\boldsymbol{\xi}$ and $\delta\boldsymbol{\theta}$ be respectively the rotation angle, rotation axis and axis-angle associated with the error attitude $\delta\mathbf{R}$ such that $\delta\boldsymbol{\theta} = \delta\theta \cdot \boldsymbol{\xi}$ and $\delta\mathbf{R} = \exp\left((\delta\boldsymbol{\theta})_\times\right)$, then (25a) can be rewritten as

$$\exp\left((\delta\boldsymbol{\theta}_\tau)_\times\right) = \exp\left(-(\widehat{\boldsymbol{\omega}}_{\tau-1|k-1})_\times \Delta t\right) \exp\left((\delta\boldsymbol{\theta}_{\tau-1})_\times\right) \exp\left((\widehat{\boldsymbol{\omega}}_{\tau-1|k-1} - \Delta\mathbf{b}_{\tau-1} - \mathbf{n}_{r_{\tau-1}})_\times \Delta t\right) \tag{26}$$

Equation (26) is the exact nonlinear error state equation. This extremely nonlinear state equation can be linearized by assuming the error state being small, which leads to

$$\delta\mathbf{R} = \exp\left(\delta\boldsymbol{\theta}_\times\right) \approx \mathbf{I}_{3\times 3} + (\delta\boldsymbol{\theta})_\times \tag{27}$$

Substituting (27) into (26) and neglecting higher order terms yields the linearized error state equation as follows:

$$\begin{bmatrix}\delta\boldsymbol{\theta}_\tau \\ \Delta\mathbf{b}_\tau\end{bmatrix} = \begin{bmatrix}\exp\left(-(\widehat{\boldsymbol{\omega}}_{\tau-1|k-1}\Delta t)_\times\right) & -\mathbf{M}(\widehat{\boldsymbol{\omega}}_{\tau-1|k-1}\Delta t)\Delta t \\ \mathbf{0}_{3\times 3} & \mathbf{I}_{3\times 3}\end{bmatrix} \cdot \begin{bmatrix}\delta\boldsymbol{\theta}_{\tau-1} \\ \Delta\mathbf{b}_{\tau-1}\end{bmatrix} + \begin{bmatrix}-\mathbf{M}(\widehat{\boldsymbol{\omega}}_{\tau-1|k-1}\Delta t)\Delta t & \mathbf{0}_{3\times 3} \\ \mathbf{0}_{3\times 3} & \mathbf{I}_{3\times 3}\Delta t\end{bmatrix} \begin{bmatrix}\mathbf{n}_{r_{\tau-1}} \\ \mathbf{n}_{w_{\tau-1}}\end{bmatrix} \tag{28}$$

where $\mathbf{w}(\tau-1) \sim \mathcal{N}(\mathbf{0}, \mathcal{Q}(\tau-1))$, $\tau \geq k$, meaning that the error system starts from the previous time step $k-1$, and $\mathbf{M}(\cdot)$ takes the definitions of (15). For MEMS gyros concerned in this paper, the sampling rate is quite high (e.g. up to several kHz), second order terms $(\Delta t)^2$ can be safely neglected, which leads to $\mathbf{M}(\widehat{\boldsymbol{\omega}}_{\tau-1|k-1}\Delta t)\Delta t \approx \mathbf{I}_{3\times 3}\Delta t$. In practice, the linearized error system in (28) can be simplified as

$$\underbrace{\begin{bmatrix}\delta\boldsymbol{\theta}_\tau \\ \Delta\mathbf{b}_\tau\end{bmatrix}}_{\mathbf{x}_\tau} = \underbrace{\begin{bmatrix}\exp\left(-(\widehat{\boldsymbol{\omega}}_{\tau-1|k-1}\Delta t)_\times\right) & -\mathbf{I}_{3\times 3}\Delta t \\ \mathbf{0}_{3\times 3} & \mathbf{I}_{3\times 3}\end{bmatrix}}_{\mathbf{F}_{\tau-1}} \underbrace{\begin{bmatrix}\delta\boldsymbol{\theta}_{\tau-1} \\ \Delta\mathbf{b}_{\tau-1}\end{bmatrix}}_{\mathbf{x}_{\tau-1}} + \underbrace{\begin{bmatrix}-\mathbf{I}_{3\times 3}\Delta t & \mathbf{0}_{3\times 3} \\ \mathbf{0}_{3\times 3} & \mathbf{I}_{3\times 3}\Delta t\end{bmatrix}}_{\mathbf{B}_w} \underbrace{\begin{bmatrix}\mathbf{n}_{r_{\tau-1}} \\ \mathbf{n}_{w_{\tau-1}}\end{bmatrix}}_{\mathbf{w}_{\tau-1}} \tag{29}$$

The indirect extended Kalman filter, as its name implies, propagates the error state and the associated covariance matrix by the linearized state equation (29) instead of the original system equation (18). When the attitude measurements are received at a lower rate than that of the gyro, there are multiple gyro measurements in between two consecutive attitude measurements. In this case, as the error system (29) is defined over all time steps $\tau \geq k-1$, it enables the state and covariance matrix to keep propagating from previous measurement at time step $k-1$ until the next measurement is received.

Without loss of generality, we assume the attitude measurement is at the same rate of gyro. That is, the attitude measurement is received at each gyro sample. In this case, we would only be required to propagate the state and covariance matrix by one step forward (i.e. to step k), where new attitude measurement is received and used to update the propagated state estimate. Applying the stand Kalman filter procedure to (29), which is a time varying linear system, and using the fact from (24), we have the error state and covariance matrix propagation respectively as follows:

$$\widehat{\mathbf{X}}_{k|k-1} = \mathbf{F}_{k-1}\widehat{\mathbf{X}}_{k-1|k-1} = \mathbf{0}_{6\times 1} \tag{30a}$$

$$\mathbf{P}_{k|k-1} = \mathbf{F}_{k-1}\mathbf{P}_{k-1|k-1}\mathbf{F}_{k-1}^T + \mathbf{B}_w\mathcal{Q}_{k-1}\mathbf{B}_w^T \tag{30b}$$

C. Update of The Error State System

Next, to derive the output equation, the standard EKF assumes that the attitude $\mathbf{R}$ is directly measurable, either by the combination of an accelerometer and a magnetometer or by other means. Denote $\mathbf{R}_m$ be the attitude measurement, $\mathbf{R}_m$ is generally modeled as

$$\mathbf{R}_m = \mathbf{R}\mathbf{R}_n \tag{31}$$

where $\mathbf{R}_n$ is the measurement noise, which is very small and assumed as $\mathbf{R}_n = \exp(\mathbf{v}_\times)$, $\mathbf{v} \sim \mathcal{N}(\mathbf{0}, \mathcal{R})$ is the axis-angle representation of the measurement noise $\mathbf{R}_n$.

The output in the standard EKF, at the time step k, is then defined as exponential coordinate of the error attitude between the measurement and the most recent estimate (i.e. the a-priori estimate)

$$\mathbf{Z}_k = \left(\log\left(\widehat{\mathbf{R}}_{k|k-1}^T \mathbf{R}_{m_k}\right)\right)_\vee \tag{32}$$

where $\log(\cdot)$ is the matrix logarithm map.

Substituting (22a) and (31) into (32) and neglecting higher order terms such as $\delta\boldsymbol{\theta}_k \times \mathbf{v}_k$, we obtain the output equation as below

$$\mathbf{Z}_k = \underbrace{\begin{bmatrix}\mathbf{I}_{3\times3} & \mathbf{0}_{3\times3}\end{bmatrix}}_{\mathbf{H}_k} \begin{bmatrix}\delta\boldsymbol{\theta}_k \\ \Delta\mathbf{b}_k\end{bmatrix} + \mathbf{v}_k \tag{33}$$

Recalling (30) and following the standard Kalman filter procedure, we obtain the update of the error state system as below

$$\mathbf{S}_k = \mathbf{H}_k\mathbf{P}_{k|k-1}\mathbf{H}_k^T + \mathcal{R}_k \tag{34a}$$
$$\mathbf{K}_k = \mathbf{P}_{k|k-1}\mathbf{H}_k^T\mathbf{S}_k^{-1} \tag{34b}$$
$$\widehat{\mathbf{X}}_{k|k} = \mathbf{K}_k\mathbf{Z}_k \tag{34c}$$
$$\mathbf{P}_{k|k} = (\mathbf{I}_{6\times6} - \mathbf{K}_k\mathbf{H}_k)\mathbf{P}_{k|k-1} \tag{34d}$$

Therefore, we have

$$\delta\widehat{\boldsymbol{\theta}}_{k|k} = \mathbf{S}_1\mathbf{K}_k\mathbf{Z}_k \tag{35a}$$
$$\Delta\widehat{\mathbf{b}}_{k|k} = \mathbf{S}_2\mathbf{K}_k\mathbf{Z}_k \tag{35b}$$

where $\mathbf{S}_1 = [\mathbf{I}_{3\times3}\ \mathbf{0}_{3\times3}]$ and $\mathbf{S}_1 = [\mathbf{0}_{3\times3}\ \mathbf{I}_{3\times3}]$.

D. Update of The Primal System

After obtaining the prediction and update of the error state system respectively given in (30) and (34), the next is to derive the update step of the primal system. Again, recalling the definition in (22), we have

$$\mathbf{R}_k = \widehat{\mathbf{R}}_{k|k-1}\delta\mathbf{R}_k \tag{36a}$$
$$\mathbf{b}_k = \widehat{\mathbf{b}}_{k|k-1} + \Delta\mathbf{b}_k \tag{36b}$$

which leads to the estimate respectively shown as below

$$\widehat{\mathbf{R}}_{k|k} = \widehat{\mathbf{R}}_{k|k-1}\delta\widehat{\mathbf{R}}_{k|k} \tag{37a}$$
$$\widehat{\mathbf{b}}_{k|k} = \widehat{\mathbf{b}}_{k|k-1} + \Delta\widehat{\mathbf{b}}_{k|k} \tag{37b}$$

Substituting (35) into the above equation yields

$$\widehat{\mathbf{R}}_{k|k} = \widehat{\mathbf{R}}_{k|k-1}\exp\left((\mathbf{S}_1\mathbf{K}_k\mathbf{Z}_k)_\times\right) \tag{38a}$$
$$\widehat{\mathbf{b}}_{k|k} = \widehat{\mathbf{b}}_{k|k-1} + \mathbf{S}_2\mathbf{K}_k\mathbf{Z}_k \tag{38b}$$

E. The Indirect EKF Algorithm on $SO(3)$

Finally, the complete indirect extended Kalman filter on $SO(3)$ can be summarized in **Algorithm. 1**.

Algorithm 1 Indirect EKF algorithm on $SO(3)$

Initialization: $\widehat{\mathbf{R}}_{0|-1} = \mathbf{E}[\mathbf{R}_0]$; $\widehat{\mathbf{b}}_{0|-1} = \mathbf{b}_0; \mathbf{P}_{0|-1} = \mathbf{P}_0$
for k = 0, 1, 2, ... ,N **do**
Receive the attitude measurement $\mathbf{R}_{m_k}$
Update:
$\mathbf{Z}_k = \left(\log\left(\widehat{\mathbf{R}}_{k|k-1}^T\mathbf{R}_{m_k}\right)\right)_\vee$
$\mathbf{S}_k = \mathbf{H}_k\mathbf{P}_{k|k-1}\mathbf{H}_k^T + \mathcal{R}_k$
$\mathbf{K}_k = \mathbf{P}_{k|k-1}\mathbf{H}_k^T\mathbf{S}_k^{-1}$
$\widehat{\mathbf{R}}_{k|k} = \widehat{\mathbf{R}}_{k|k-1}\exp\left((\mathbf{S}_1\mathbf{K}_k\mathbf{Z}_k)_\times\right)$
$\widehat{\mathbf{b}}_{k|k} = \widehat{\mathbf{b}}_{k|k-1} + \mathbf{S}_2\mathbf{K}_k\mathbf{Z}_k$
$\mathbf{P}_{k|k} = (\mathbf{I}_{6\times6} - \mathbf{K}_k\mathbf{H}_k)\mathbf{P}_{k|k-1}$
Predict:
$\widehat{\boldsymbol{\omega}}_{k|k} = \boldsymbol{\omega}_{m_k} - \widehat{\mathbf{b}}_{k|k}$
$\widehat{\mathbf{R}}_{k+1|k} = \widehat{\mathbf{R}}_{k|k}\exp\left((\widehat{\boldsymbol{\omega}}_{k|k})_\times\Delta t\right)$
$\widehat{\mathbf{b}}_{k+1|k} = \widehat{\mathbf{b}}_{k|k}$
$\mathbf{P}_{k+1|k} = \mathbf{F}_k\mathbf{P}_{k|k}\mathbf{F}_k^T + \mathbf{B}_w\mathcal{Q}_k\mathbf{B}_w^T$
end for

IV. Indirect EKF with The Notch Filter

As mentioned in the introduction, the translational vibration considerably contaminates the accelerometer measurement, usually leading to poor attitude estimation based on the indirect EKF algorithm presented previously. Since the frequency range of such noise is narrow, we apply a notch filter to attenuate the vibration noise. The transfer function of a notch filter in discrete time domain is represented as

$$G_f(z) = \frac{z^2 - 2\alpha\cos(\omega_0\Delta t)z + \alpha^2}{z^2 - 2\beta\cos(\omega_0\Delta t))z + \beta^2} \tag{39}$$

where z is the $\mathcal{Z}$-transform variable, Δt is the sampling time as before, ω_0 is the dominant noise frequency, α and β are damping ratio-like parameters that are used to tune the width and depth of the notch filter. Fig. 1 shows the Bode plot of a typical notch filter with $\alpha = 1$, $\beta = 0.7$ and $\omega_0 = 10Hz$. It is seen that such a notch filter achieves 150dB attenuation around the frequency ω_0, considerably mitigating the effect of vibration noise.

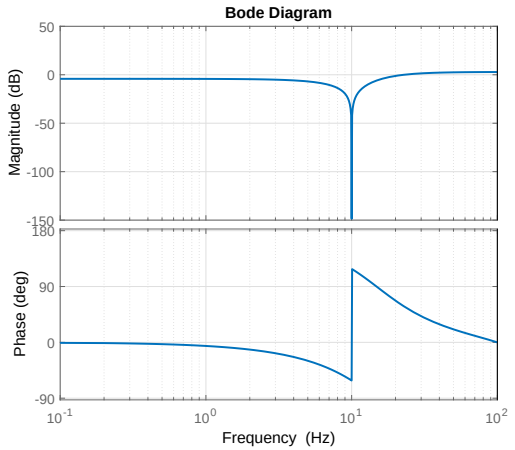

Fig. 1. Bode diagram of a notch filter with $\alpha = 1.0, \beta = 0.7$ and $\omega_0 = 10Hz$, sampling frequency is $200Hz$

The employed notch filter can be explicitly represented by a linear state space model, known as state space realization [26]

$$\begin{aligned}\mathbf{x}_{f_k} &= \mathbf{A}\mathbf{x}_{f_{k-1}} + \mathbf{B}\left(\mathbf{a}_{m_{k-1}} - \mathbf{a}_{c_{k-1}}\right) \\ \mathbf{a}_{f_k} &= \mathbf{C}\mathbf{x}_{f_k} + \mathbf{D}\left(\mathbf{a}_{m_k} - \mathbf{a}_{c_k}\right)\end{aligned} \tag{40}$$

where $\mathbf{x}_f$ is the state of the notch filter, $\mathbf{a}_{m_k} - \mathbf{a}_{c_k}$ is the accelerometer raw measurements compensated by translational acceleration, and $\mathbf{a}_{f_k}$ is the filtered accelerometer readings, which will be fed into the indirect EKF for attitude and bias estimation. Assume the notch filter for each channel is order of N, then $\mathbf{A} \in \mathbb{R}^{3N\times 3N}$; $\mathbf{B} \in \mathbb{R}^{3N\times 3}$; $\mathbf{C} \in \mathbb{R}^{3\times 3N}$ and $\mathbf{D} \in \mathbb{R}^{3\times 3}$

Shown in Fig. 1, due to the large attenuation around the notch frequency ω_0, which is the dominant frequency components of the narrowband noise, the filtered accelerometer measurements will be susceptible to no such vibration noise. However, Fig. 1 shows that the added notch filter introduces significant delay to the input signal, which in turn potentially leads to overshoot or even divergence in attitude control.

To eliminate the delay, we regard the added notch filter as a part of the original system and form an augmented system model. We then explicitly incorporate the notch filter dynamics in the state observer. In the case of linear system, the augmented system will remain observable and the resulting Kalman filter will therefore converge to ground truth state. Proving the observability of the augmented system is, however, out of the scope of this paper. Furthermore, due to the large attenuation of the notch filter, the narrow-band vibration noise shows no effect on the filter output and can be removed from the accelerometer model in (19b). As a result, the augmented system can be written as

$$\begin{aligned}
\mathbf{R}_k &= \mathbf{R}_{k-1}\exp\left((\boldsymbol{\omega}_{k-1})_\times \Delta t\right) && \text{(41a)}\\
\boldsymbol{\omega}_{k-1} &= \boldsymbol{\omega}_{m_{k-1}} - \mathbf{b}_{k-1} - \mathbf{n}_{r_{k-1}} &&\\
\mathbf{b}_k &= \mathbf{b}_{k-1} + \mathbf{n}_{w_{k-1}}\Delta t && \text{(41b)}\\
\mathbf{x}_{f_k} &= \mathbf{A}\mathbf{x}_{f_{k-1}} + \mathbf{B}\left(\mathbf{a}_{m_{k-1}} - \mathbf{a}_{c_{k-1}}\right) && \text{(41c)}\\
\mathbf{a}_{m_{k-1}} &= -\mathbf{g}_{k-1} + \mathbf{a}_{c_{k-1}} + \mathbf{n}_{a_{k-1}} &&
\end{aligned}$$

To linearize the augmented system similar to the standard EKF case, we predict the augmented states based on all the outputs up to $k-1$ by the following system

$$\widehat{\mathbf{x}}_{f_{\tau|k-1}} = \mathbf{A}\widehat{\mathbf{x}}_{f_{\tau-1|k-1}} - \mathbf{B}\widehat{\mathbf{R}}^T_{\tau-1|k-1}\mathbf{e}_3;\quad \tau \geq k \quad (42)$$

The prediction of attitude and gyro bias is identical to (23).

Following the standard EKF case, we define the error filter state $\Delta\mathbf{x}_f$ as the deviation between the predicted filter state $\widehat{\mathbf{x}}_{f_{\tau|k-1}}$ and its true value $\mathbf{x}_{f_\tau}$

$$\Delta\mathbf{x}_{f_\tau} = \mathbf{x}_{f_\tau} - \widehat{\mathbf{x}}_{f_{\tau|k-1}} \quad (43)$$

Substituting (41c), (42) and (22) into (43), one can obtain

$$\begin{aligned}
\Delta\mathbf{x}_{f_\tau} = \mathbf{A}\Delta\mathbf{x}_{f_{\tau-1}} &- \mathbf{B}\left(\widehat{\mathbf{R}}^T_{\tau-1|k-1}\mathbf{e}_3\right)_\times \delta\boldsymbol{\theta}_{\tau-1}\\
&+ \mathbf{B}\mathbf{n}_{a_{\tau-1}} \quad (44)
\end{aligned}$$

Therefore, the augmented system represented by its error state can be written as

$$\begin{aligned}
\underbrace{\begin{bmatrix}\delta\boldsymbol{\theta}_\tau\\ \Delta\mathbf{b}_\tau\\ \Delta\mathbf{x}_{f_\tau}\end{bmatrix}}_{\overline{\mathbf{X}}(\tau)} &= \underbrace{\begin{bmatrix}\exp\left(-(\widehat{\boldsymbol{\omega}}_{\tau-1|k-1})_\times\Delta t\right) & -\mathbf{I}_{3\times3}\Delta t & \mathbf{0}_{3\times3N}\\ \mathbf{0}_{3\times3} & \mathbf{I}_{3\times3} & \mathbf{0}_{3\times3N}\\ -\mathbf{B}\left(\widehat{\mathbf{R}}^T_{\tau-1|k-1}\mathbf{e}_3\right)_\times & \mathbf{0}_{3N\times3} & \mathbf{A}\end{bmatrix}}_{\overline{\mathbf{F}}_{\tau-1}}\\
&\cdot \underbrace{\begin{bmatrix}\delta\boldsymbol{\theta}_{\tau-1}\\ \Delta\mathbf{b}_{\tau-1}\\ \Delta\mathbf{x}_{f_{\tau-1}}\end{bmatrix}}_{\overline{\mathbf{X}}_{\tau-1}} + \underbrace{\begin{bmatrix}-\mathbf{I}_{3\times3}\Delta t & \mathbf{0}_{3\times3} & \mathbf{0}_{3\times3}\\ \mathbf{0}_{3\times3} & \mathbf{I}_{3\times3}\Delta t & \mathbf{0}_{3\times3}\\ \mathbf{0}_{3N\times3} & \mathbf{0}_{3N\times3} & \mathbf{B}\end{bmatrix}}_{\overline{\mathbf{B}}_w}\underbrace{\begin{bmatrix}\mathbf{n}_{r_{\tau-1}}\\ \mathbf{n}_{w_{\tau-1}}\\ \mathbf{n}_{a_{\tau-1}}\end{bmatrix}}_{\overline{\mathbf{w}}_{\tau-1}} \quad (45)
\end{aligned}$$

where $\overline{\mathbf{w}}(\tau-1) \sim \mathcal{N}(\mathbf{0}, \overline{\mathcal{Q}}(\tau-1))$, and $\tau \geq k$.

Implied by (43), we have $\Delta\mathbf{x}_{f_{k-1|k-1}} = \mathbf{x}_{f_{k-1|k-1}} - \mathbf{x}_{f_{k-1|k-1}} = \mathbf{0}_{3N\times1}$ and $\widehat{\overline{\mathbf{X}}}_{k-1|k-1} = \mathbf{0}_{(3N+6)\times1}$. Similar to the standard EKF case, we assume the attitude measurement is at the same rate of gyro and would be only required to propagate for one step forward:

$$\begin{aligned}
\widehat{\overline{\mathbf{X}}}_{k|k-1} &= \overline{\mathbf{F}}_{k-1}\widehat{\overline{\mathbf{X}}}_{k-1|k-1} = \mathbf{0}_{(3N+6)\times1} && \text{(46a)}\\
\overline{\mathbf{P}}_{k|k-1} &= \overline{\mathbf{F}}_{k-1}\overline{\mathbf{P}}_{k-1|k-1}\overline{\mathbf{F}}^T_{k-1} + \overline{\mathbf{B}}_w\overline{\mathcal{Q}}_{k-1}\overline{\mathbf{B}}^T_w && \text{(46b)}
\end{aligned}$$

Next, the measurements of the augmented system are the filtered accelerometer signal and the yaw measurement, i.e,

$$\begin{aligned}
\mathbf{a}_{f_k} &= \mathbf{C}\mathbf{x}_{f_k} + \mathbf{D}\left(\mathbf{a}_{m_k} - \mathbf{a}_{c_k}\right) && \text{(47a)}\\
\psi_{m_k} &= \psi_k + n_{y_k} && \text{(47b)}
\end{aligned}$$

The output of the augmented system is then defined as

$$\overline{\mathbf{Z}}_k = \begin{bmatrix}\mathbf{a}_{f_k} - \widehat{\mathbf{a}}_{f_{k|k-1}}\\ \psi_{m_k} - \widehat{\psi}_{k|k-1}\end{bmatrix};\quad \tau \geq k \quad (48)$$

where $\widehat{\mathbf{a}}_f$ and $\widehat{\psi}$ are respectively the predicted filter output and the predicted yaw angle, i.e.,

$$\begin{aligned}
\widehat{\mathbf{a}}_{f_{k|k-1}} &= \mathbf{C}\widehat{\mathbf{x}}_{f_{k|k-1}} - \mathbf{D}\widehat{\mathbf{R}}^T_{k|k-1}\mathbf{e}_3 && \text{(49a)}\\
\widehat{\psi}_{k|k-1} &= -\arctan\frac{\mathbf{e}_1^T\widehat{\mathbf{R}}_{k|k-1}\mathbf{e}_2}{\mathbf{e}_2^T\widehat{\mathbf{R}}_{k|k-1}\mathbf{e}_2} && \text{(49b)}
\end{aligned}$$

Substituting (47) and (49) into (48) produces

$$\begin{aligned}
\overline{\mathbf{Z}}_k = &\underbrace{\begin{bmatrix}-\mathbf{D}\left(\widehat{\mathbf{R}}^T_{k|k-1}\mathbf{e}_3\right)_\times & \mathbf{0}_{3\times3} & \mathbf{C}\\ \mathbf{H}_{f_k} & \mathbf{0}_{1\times3} & \mathbf{0}_{1\times3N}\end{bmatrix}}_{\overline{\mathbf{H}}_k}\underbrace{\begin{bmatrix}\delta\boldsymbol{\theta}_k\\ \Delta\mathbf{b}_k\\ \Delta\mathbf{x}_{f_k}\end{bmatrix}}_{\overline{\mathbf{X}}_k}\\
&+ \underbrace{\begin{bmatrix}\mathbf{D} & \mathbf{0}_{3\times1}\\ 0 & 1\end{bmatrix}}_{\overline{\mathbf{D}}_v}\underbrace{\begin{bmatrix}\mathbf{n}_{a_k}\\ n_{y_k}\end{bmatrix}}_{\overline{\mathbf{v}}_k} \quad (50)
\end{aligned}$$

where $\overline{\mathbf{v}}_k \sim \mathcal{N}(\mathbf{0}, \overline{\mathcal{R}}_k)$ and

$$\mathbf{H}_f = \begin{bmatrix}\frac{\widehat{r}_{23}\widehat{r}_{12}-\widehat{r}_{13}\widehat{r}_{22}}{\widehat{r}^2_{12}+\widehat{r}^2_{22}} & 0 & \frac{\widehat{r}_{11}\widehat{r}_{22}-\widehat{r}_{21}\widehat{r}_{12}}{\widehat{r}^2_{12}+\widehat{r}^2_{22}}\end{bmatrix} \quad (51)$$

$\widehat{r}_{ij}$ is the i-th row j-th column element of matrix $\widehat{\mathbf{R}}_{k|k-1}$.

Similar to the standard indirect EKF case, recalling (46) and following the standard Kalman filter procedure, we obtain the update of the augmented error state system

$$\begin{aligned}
\overline{\mathbf{S}}_k &= \overline{\mathbf{H}}_k\overline{\mathbf{P}}_{k|k-1}\overline{\mathbf{H}}^T_k + \overline{\mathbf{D}}_v\overline{\mathcal{R}}_k\overline{\mathbf{D}}^T_v && \text{(52a)}\\
\overline{\mathbf{K}}_k &= \overline{\mathbf{P}}_{k|k-1}\overline{\mathbf{H}}^T_k\overline{\mathbf{S}}^{-1}_k && \text{(52b)}\\
\widehat{\overline{\mathbf{X}}}_{k|k} &= \overline{\mathbf{K}}_k\overline{\mathbf{Z}}_k && \text{(52c)}\\
\overline{\mathbf{P}}_{k|k} &= (\mathbf{I}_{(3N+6)\times(3N+6)} - \overline{\mathbf{K}}_k\overline{\mathbf{H}}_k)\overline{\mathbf{P}}_{k|k-1} && \text{(52d)}
\end{aligned}$$

Therefore, we have

$$\begin{aligned}
\delta\widehat{\boldsymbol{\theta}}_{k|k} &= \overline{\mathbf{S}}_1\overline{\mathbf{K}}_k\overline{\mathbf{Z}}_k && \text{(53a)}\\
\Delta\widehat{\mathbf{b}}_{k|k} &= \overline{\mathbf{S}}_2\overline{\mathbf{K}}_k\overline{\mathbf{Z}}_k && \text{(53b)}\\
\Delta\widehat{\mathbf{x}}_{f_{k|k}} &= \overline{\mathbf{S}}_3\overline{\mathbf{K}}_k\overline{\mathbf{Z}}_k && \text{(53c)}
\end{aligned}$$

where $\overline{\mathbf{S}}_1 = [\mathbf{I}_{3\times3}\ \mathbf{0}_{3\times3}\ \mathbf{0}_{3\times3N}]$, $\overline{\mathbf{S}}_2 = [\mathbf{0}_{3\times3}\ \mathbf{I}_{3\times3}\ \mathbf{0}_{3\times3N}]$ and $\overline{\mathbf{S}}_3 = [\mathbf{0}_{3N\times3}\ \ \mathbf{0}_{3N\times3}\ \ \mathbf{I}_{3N\times3N}]$.

Finally, the complete indirect extended Kalman filter with a notch filter can be summarized in **Algorithm. 2**.

Algorithm 2 Indirect EKF algorithm with Notch Filter

Initialization: $\widehat{\mathbf{R}}_{0|-1} = \mathbf{E}[\mathbf{R}_0]$; $\widehat{\mathbf{b}}_{0|-1} = \mathbf{E}[\mathbf{b}_0]$; $\widehat{\mathbf{x}}_{f_{0|-1}} = \mathbf{x}_{f_0}$; $\mathbf{P}_{0|-1} = \mathbf{P}_0$

for k = 0, 1, 2,..., n **do**

Receive the measurements a_{m_k} and ψ_{m_k}

Notch Filter

Filter output:

$$\mathbf{a}_{f_k} = \mathbf{C}\mathbf{x}_{f_k} + \mathbf{D}\left(\mathbf{a}_{m_k} - \mathbf{a}_{c_k}\right)$$

State update:

$$\mathbf{x}_{f_{k+1}} = \mathbf{A}\mathbf{x}_{f_k} + \mathbf{B}\left(\mathbf{a}_{m_k} - \mathbf{a}_{c_k}\right)$$

Extended Kalman Filter

Update:

$$\widehat{\mathbf{a}}_{f_{k|k-1}} = \mathbf{C}\widehat{\mathbf{x}}_{f_{k|k-1}} - \mathbf{D}\widehat{\mathbf{R}}^T_{k|k-1}\mathbf{e}_3$$

$$\widehat{\psi}_{k|k-1} = -\arctan\frac{\mathbf{e}_1^T\widehat{\mathbf{R}}_{k|k-1}\mathbf{e}_2}{\mathbf{e}_2^T\widehat{\mathbf{R}}_{k|k-1}\mathbf{e}_2}$$

$$\overline{\mathbf{Z}}_k = \begin{bmatrix} \mathbf{a}_{f_k} - \widehat{\mathbf{a}}_{f_{k|k-1}} & \psi_{m_k} - \widehat{\psi}_{k|k-1} \end{bmatrix}^T$$

$$\overline{\mathbf{S}}_k = \overline{\mathbf{H}}_k\overline{\mathbf{P}}_{k|k-1}\overline{\mathbf{H}}_k^T + \overline{\mathbf{D}}_v\overline{\mathcal{R}}_k\overline{\mathbf{D}}_v^T$$

$$\overline{\mathbf{K}}_k = \overline{\mathbf{P}}_{k|k-1}\overline{\mathbf{H}}_k^T\overline{\mathbf{S}}_k^{-1}$$

$$\widehat{\mathbf{R}}_{k|k} = \widehat{\mathbf{R}}_{k|k-1}\exp\left((\overline{\mathbf{S}}_1\overline{\mathbf{K}}_k\overline{\mathbf{Z}}_k)_\times\right)$$

$$\widehat{\mathbf{b}}_{k|k} = \widehat{\mathbf{b}}_{k|k-1} + \overline{\mathbf{S}}_2\overline{\mathbf{K}}_k\overline{\mathbf{Z}}_k$$

$$\widehat{\mathbf{x}}_{f_{k|k}} = \widehat{\mathbf{x}}_{f_{k|k-1}} + \overline{\mathbf{S}}_3\overline{\mathbf{K}}_k\overline{\mathbf{Z}}_k$$

$$\overline{\mathbf{P}}_{k|k} = (\mathbf{I}_{(3N+6)\times(3N+6)} - \overline{\mathbf{K}}_k\overline{\mathbf{H}}_k)\overline{\mathbf{P}}_{k|k-1}$$

Predict:

$$\widehat{\boldsymbol{\omega}}_{k|k} = \boldsymbol{\omega}_{m_k} - \widehat{\mathbf{b}}_{k|k}$$

$$\widehat{\mathbf{R}}_{k+1|k} = \widehat{\mathbf{R}}_{k|k}\exp\left((\widehat{\boldsymbol{\omega}}_{k|k})_\times\Delta t\right)$$

$$\widehat{\mathbf{b}}_{k+1|k} = \widehat{\mathbf{b}}_{k|k}$$

$$\widehat{\mathbf{x}}_{f_{k+1|k}} = \mathbf{A}\widehat{\mathbf{x}}_{f_{k|k}} - \mathbf{B}\widehat{\mathbf{R}}^T_{k|k}\mathbf{e}_3$$

$$\overline{\mathbf{P}}_{k+1|k} = \overline{\mathbf{F}}_k\overline{\mathbf{P}}_{k|k}\overline{\mathbf{F}}_k^T + \overline{\mathbf{B}}_w\overline{\mathcal{Q}}_k\overline{\mathbf{B}}_w^T$$

end for

V. Adaptive Noise Frequency Estimation

As the dominant noise frequency usually drifts over time or over the environment, it is necessary to identify the noise frequency in real time and tune the notch frequency accordingly. We adopt the adaptive frequency estimation scheme proposed by Jia in [17]. Assume the noise dominant frequency is ω_0, then the vibration noise d can be written as

$$d_k = A\sin(\omega_0 k\Delta t + \varphi) \tag{54}$$

where A, φ are respectively the amplitude and phase of the dominant noise.

Using the parameterization in (54), we can prove that the following relation holds

$$d_k - \eta d_{k-1} + d_{k-2} = 0 \tag{55}$$

where $\eta = 2\cos(\omega_0\Delta t)$. The residual error for a candidate η is then defined as

$$\varepsilon_k(\eta) = d_k - (\eta d_{k-1} - d_{k-2}) \tag{56}$$

In [17], a Least Mean Square (LMS) is utilized to estimate η in real time, i.e.,

$$\begin{aligned}\widehat{\eta}_{k+1} &= \widehat{\eta}_k - \lambda\left.\frac{\partial\varepsilon_k^2(\eta)}{\partial\eta}\right|_{\widehat{\eta}_k} \\ &= \widehat{\eta}_k + \lambda d_{k-1}\varepsilon_k(\widehat{\eta}_k)\end{aligned} \tag{57}$$

where λ is the adaptation gain. The estimated $\widehat{\eta}_{k+1}$ can be directly used in (39) to construct the notch filter in real time, forming an adaptive notch filter, and also in (45) and (50) to update the system matrix (i.e. $\mathbf{A}, \mathbf{B}, \mathbf{C}$ and $\mathbf{D}$) used in EKF.

One problem with the frequency estimation method in (57) is that, it requires to know the vibration noise d, which is apparently not measurable in the actual system. In this work, we estimate dominant noise frequency (i.e. η) from the reconstructed vibration noise signal. Recalling the accelerometer model (19b), the actual vibration noise can be rewritten as

$$\mathbf{d}_k = \mathbf{a}_{m_k} + \mathbf{g}_k - \mathbf{a}_{c_k} - \mathbf{n}_{a_k} \tag{58}$$

Accordingly, the reconstructed vibration noise can be obtained as follows

$$\widehat{\mathbf{g}}_{k|k} = \widehat{\mathbf{R}}^T_{k|k}\mathbf{e}_3 \tag{59a}$$

$$\widehat{\mathbf{d}}_k = \mathbf{a}_{m_k} + \widehat{\mathbf{g}}_{k|k} - \mathbf{a}_{c_k} \tag{59b}$$

Furthermore, to mitigate the effect of measurement noise $\mathbf{n}_{a_k}$ and noise frequency components other than the dominant noise, a low-pass filter (or band-pass filter) is used to limit the reconstructed vibration noise $\widehat{\mathbf{d}}_k$ within a prescribed frequency range. The resulting frequency estimation algorithm is summarized in **Algorithm. 3**.

Algorithm 3 Adaptive frequency estimator

Initialization: $\lambda = \lambda_0, \widehat{\boldsymbol{\eta}}_0 = \boldsymbol{\eta}_0$

for $k = 2, 3, ..., n$ **do**

$$\widehat{\mathbf{d}}_k = \mathbf{a}_{m_k} + \widehat{\mathbf{g}}_{k|k} - \mathbf{a}_{c_k}$$

$$\widehat{\mathbf{d}}_{f_k} = LPF[\widehat{\mathbf{d}}_k]$$

$$\boldsymbol{\varepsilon}_k = \widehat{\mathbf{d}}_{f_k} + \widehat{\mathbf{d}}_{f_{k-2}} - \widehat{\boldsymbol{\eta}}_k\widehat{\mathbf{d}}_{f_{k-1}}$$

$$\widehat{\boldsymbol{\eta}}_{k+1} = \widehat{\boldsymbol{\eta}}_k + \lambda\mathbf{d}_{f_{k-1}}\boldsymbol{\varepsilon}_k$$

end for

Putting all the notch filter, augmented EKF and the adaptive frequency estimation together produces the completed algorithm, whose structure is seen in Fig. 3

VI. Application and Experiments

To verify the proposed attitude estimation algorithms, experiments are carried out on a three-axis gimbal system shown in Fig.2. The gimbal system is mounted on a host quadrotor UAV for imaging stabilization. The gimbal comprises an endpoint camera, whose attitude is to be controlled, and three joints that are actuated by three direct drive motors and can respectively rotate along the yaw, roll and pitch axis. A MEMS IMU containing a 3-axis gyro and a 3-axis accelerometer is soldered on the camera electronics rigidly to provide measurements of camera angular rate, pitch and roll angles. The yaw measurement is computed from the host vehicle attitude and the gimbal forward kinematics.

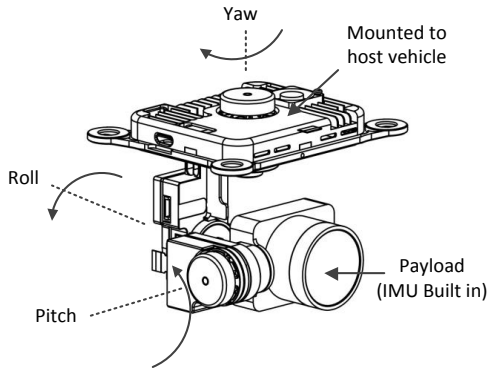

Fig. 2. Schematic of the 3-axes gimbal system (Courtesy of DJI).

For the sake of simplicity and without loss of generality, we consider the narrowband noise in only one channel, so that the

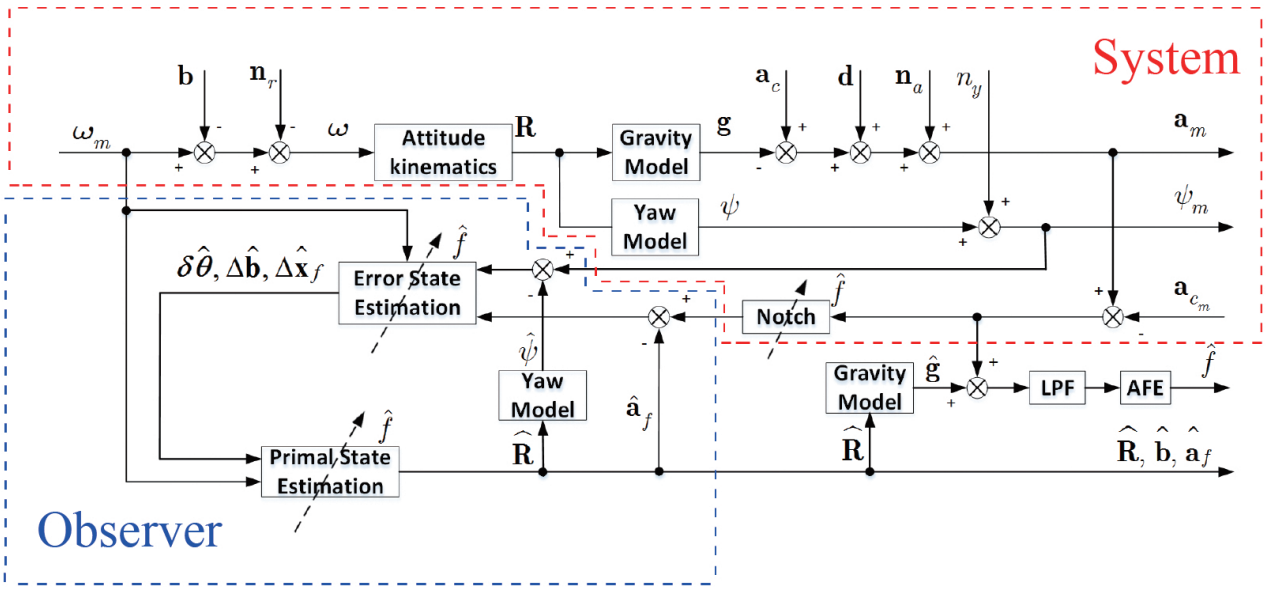

Fig. 3. Block diagram of augmented EKF with adaptive noise frequency estimation and compensation

adaptive frequency estimation and the notch filter is implemented in that channel only, and thus simplifying the augmented EKF. We conduct three experiments. In the first experiment, the standard indirect EKF (i.e. EKF not augmented with the notch filter) is implemented, and the dominant noise frequency is assumed to be known and fixed over time, thus no adaptive frequency estimation is involved and the Notch filter remains constant. A sinusoidal signal with frequency of 2 Hz and amplitude of $1g$ is intentionally added to the accelerometer measurements in channel X to simulate the vibration noise. In the second experiment, the augmented EKF is implemented to compensate the potential estimation delay brought up by the notch filter. The third experiment assumes the dominant noise frequency is unknown and drifting over time. Thus the adaptive frequency estimation module is invoked in addition to the Notch filter and augmented EKF. The complete algorithm will has its Notch filter parameter and the augmented EKF parameters adapted in real time according to the noise dominant frequency estimate.

To verify the effectiveness of the proposed attitude estimation algorithm, we examine two aspects of performance: 1) the residual error between the a-priori estimate of the observer output and their actual measurements (i.e. the vector $\bar{\mathbf{Z}}_k$ in **Algorithm. 2**). When the vibration noise is completely compensated, the measurement noise will be Gaussian white and the residual error will be mean zero according to the Kalman filter theory. 2) the error between the posterior attitude estimate $\mathbf{R}_{k|k}$ and the endpoint attitude computed by the gimbal forward kinematics. To provide accurate camera attitude measurement for comparison, the gimbal kinematic parameters are calibrated with the method in [2].

Fig. 4 shows the results of the first experiment where the standard EKF is being used. We intentionally command the gimbal system to conduct a pitch motion from zero to -90 degrees every tens of seconds to trigger the residual estimation error. From Fig. 4(a), we can see that the added Notch filter causes a considerable transient error in accelerometer x-axis (i.e. $\bar{\mathbf{Z}}_1$) every time the camera moves from zero to -90 degrees or back forth. In comparison, accelerometer y-axis (i.e. $\bar{\mathbf{Z}}_2$) suffers from no such delay since no Notch filter is added on this channel. We also notice a small transient error (within $\pm 0.8^\circ$) in yaw estimate, this is due to the residual errors in the gimbal kinematic parameters. In-depth treatment of accurate kinematic parameters identification is out of this paper

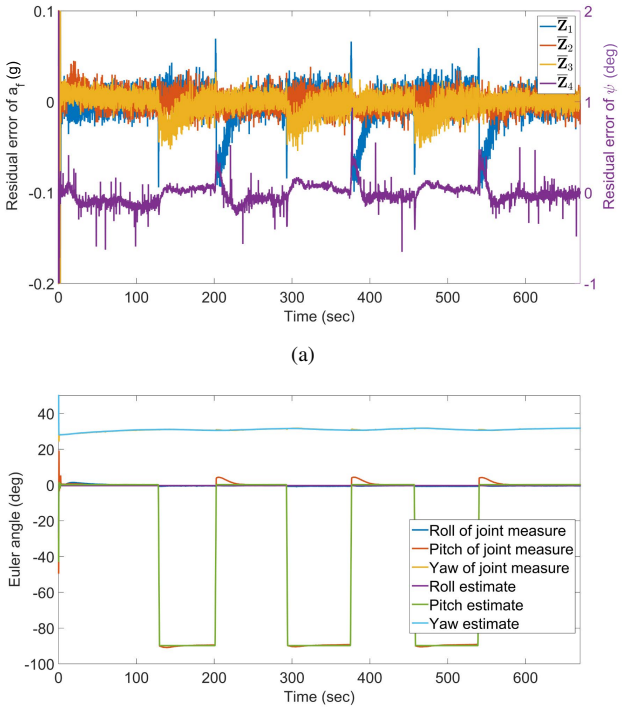

Fig. 4. Experiment 1: standard EKF concatenated with a Notch filter in the presence of narrow-band noise with known dominant frequency. (a) A-priori estimation error. (b) A-posteriori attitude estimate and attitude measurement computed from gimbal forward kinematics.

scope, readers may refer to [2] for detailed explanation. Transient error in accelerometer z-axis (i.e. $\bar{\mathbf{Z}}_3$) is caused by the error in x-axis since the accelerometer measurements are normalized to one after the translational acceleration is compensated. The estimation error in accelerometer x-axis subsequently causes a 4° overshoot in camera pitch response, as shown in Fig. 4(b). The transient response due to overshoot lasts more than 40 secs and can be clearly seen from the video captured by the camera. In Fig. 4(b), the "estimate"

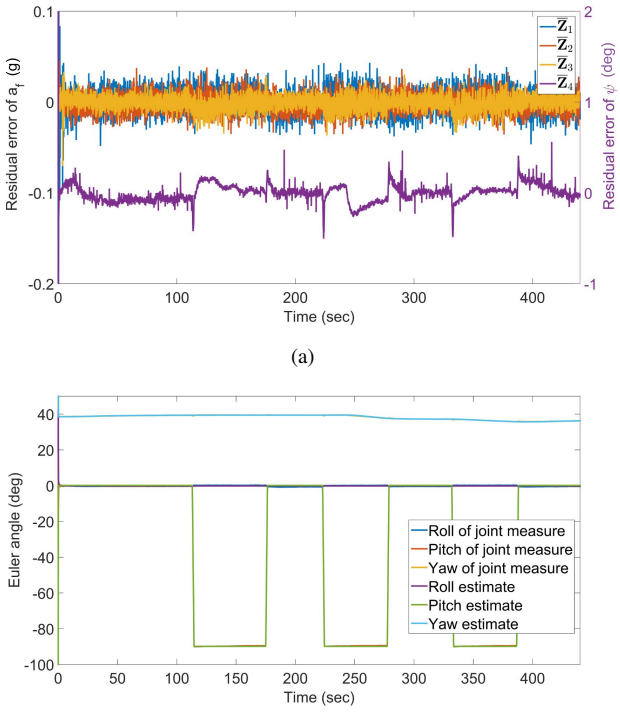

Fig. 5. Experiment 2: augment EKF concatenated with a Notch filter and in the presence of narrow-band vibration noise with known dominant frequency. (a) A-priori estimation error. (b) A-posteriori attitude estimate and attitude measurement computed from gimbal forward kinematics.

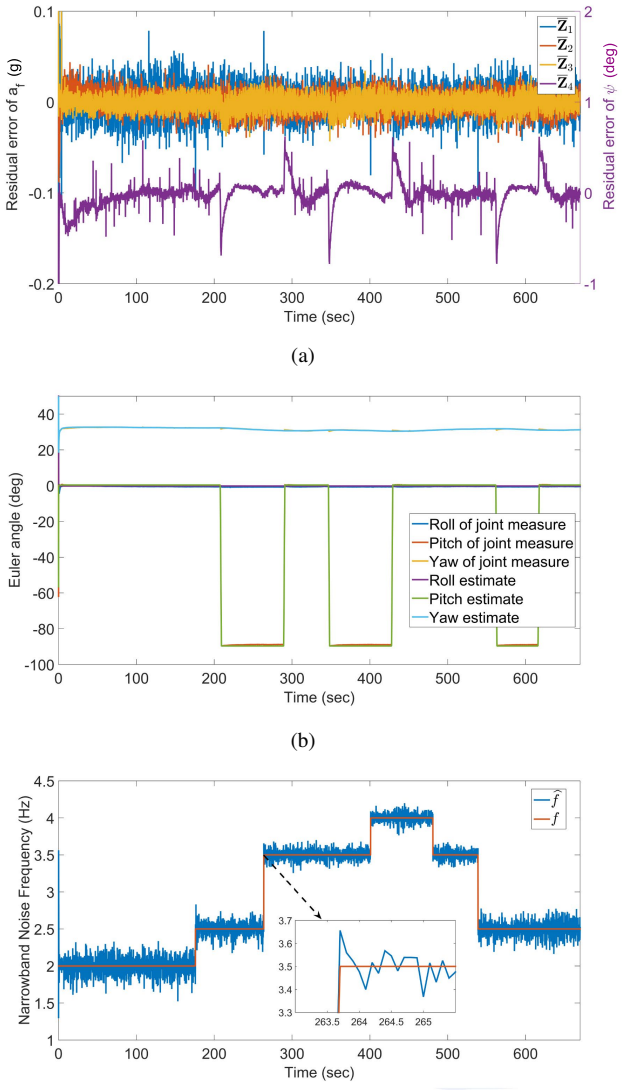

Fig. 6. Experiment 3: augmented EKF concatenated with an adaptive Notch filter in the presence of narrow-band noise with unknown and time-varying dominant frequency. (a) A-priori estimation error. (b) A-posteriori attitude estimate and attitude measurement computed from gimbal forward kinematics. (c) Estimated frequency versus the ground truth value.

refers to the attitude estimated by our proposed algorithms, and the "joint measure" refers to the attitude computed from gimbal forward kinematics. The residual error of gimbal forward kinematics is quite small, well above our required accuracy, so we can safely use the gimbal kinematics as the ground truth attitude for evaluating our proposed algorithm.

Fig. 5 shows the results of the second experiment, i.e., the augment EKF concatenated with a Notch filter and in the presence of narrow-band vibration noise with known dominant frequency. In Fig. 5(a), it is seen that the residual error for all three channels of $\mathbf{a}_f$ are almost identical even though the X channel is filtered by a notch filter, suggesting that the augmented EKF can effectively compensate the Notch filter induced delay. As a result, the three channels of $\mathbf{a}_f$ are all mean zero with negligible transient response. The resulting attitude response exhibits no nuisance overshoot, as shown in Fig. 5(b) as well as the captured video.

Finally, the results of the third are presented in Fig. 6. We intentionally change the noise dominant frequency every a few minutes to different values to test the adaptive frequency estimator as well as the EKF augmented with the proposed notch filter. In Fig. 6(c), it is seen that the estimated frequency quickly (i.e. within 0.5 sec) converges to the ground truth value. Furthermore, the residual error of the EKF, shown in Fig. 6 (a), is nearly zero mean, similar to that in the second experiment. Although in this case the residual error is slightly more noisy that of the second experiment due to the noisy frequency estimation, the estimated attitude, shown in Fig. 6(b), suffers from no such noise, narrow-band noise nor overshoot.

VII. Conclusion and Future Work

In this paper, we posed the problem of the IMU-based attitude estimation in the presence of narrow-band noise, a common problem in aerial robots due to the complicated aerodynamic effects of the robot and hostile environments they operate. An augmented EKF algorithm, based on indirect EKF framework, with a Notch filter whose notch frequency is adaptively estimated, was proposed and derived on $SO(3)$. The completed algorithm was implemented and verified on a three-axis gimbal system. The main advantage of the proposed scheme is that it effectively attenuates narrow-band noise with unknown and time-varying dominant frequency while inducing no much delay in the attitude estimate. Future work will concentrate on development of computationally efficient algorithms for compensating vibration noises with multiple narrow-bands.

References

[1] X. Lyu, H. Gu, Y. Wang, Z. Li, S. Shen and F. Zhang, "Design and implementation of a quadrotor tail-sitter VTOL UAV," in *Proc. of the IEEE Intl. Conf. on Robotics and Automation (ICRA)*, Singapore, Singapore, May 2017, pp. 3924-3930

[2] F. Zhang, "Simultaneous Self-calibration of Nonorthogonality and Nonlinearity of Cost-effective Multi-axis Inertially Stabilized Gimbal

Systems," *IEEE Robotics and Automation Letters*, vol. 3, no. 1, pp. 132-139, Jan. 2018.

[3] D. Shaeffer, "MEMS inertial sensors: A tutorial overview," *IEEE Communications Magazine* vol. 51, no. 4, pp. 100-109, Apr. 2013.

[4] R. Mahony, V. Kumar and P. Corke, "Multirotor Aerial Vehicles: Modeling, Estimation, and Control of Quadrotor," *IEEE Robotics and Automation magazine*, vol.19, no.3, pp. 20-32, Sep. 2012.

[5] R. Mahony, T. Hamel and J. Pflimlin, "Complementary filter design on the special orthogonal group SO(3)," in *Proc. of the 44th IEEE Conference on Decision and Control*, Seville, Spain, Dec. 2005, pp. 1477-1484.

[6] T. Bailey, J. Nieto, J. Guivant, M. Stevens and E. Nebot, "Consistency of EKF-SLAM Algorithm," in *Proc. Of the IEEE/RSJ Intl. Conf. on Intelligent Robots and Systems*, Beijing, China, Oct. 2006, pp. 3562-3568.

[7] M. Li and A. Mourikis, "High-precision, consistent EKF-based visual-inertial odometry," *The International Journal of Robotics Research*, vol. 32, no. 6, pp. 690-711, 2013.

[8] S. Weiss, M. Achtelik, S. Lynen, M. Chli and R. Siegwart, "Real-time onboard visual-inertial state estimation and self-calibration of MAVs in unknown environments," in *Proc. of the IEEE Intl. Conf. on Robotics and Automation*, Saint Paul, MN, USA, May 2012, pp. 957-964.

[9] G. Klein and D. Murray, "Parallel Tracking and Mapping for Small AR Workspaces," in *Proc. of the 6th IEEE and ACM Intl. Symposium on Mixed and Augmented Reality*, Nara, Japan, Nov. 2007, pp. 225-234.

[10] Smith. G.L. and Schmidt. S.F., "The Application of Statistical Filter Theory to Optimal Trajectory Determination Onbosrd a Circumlunar Vehicle," *AAS Meeting*, Reprint 61-92, Aug. 1961.

[11] J. Crassidis, F. Markley and Y. Cheng, "Survey of Nonlinear Attitude Estimation Methods," *Journal of Guidance, Control, and Dynamics*, vol. 30, no. 1, 2007.

[12] N. Trawny and S. Roumeliotis, "Indirect Kalman Filter for 3D Attitude Estimation," University of Minnesota, Dept. of Comp. Sci. & Eng, Tech. Rep. 2005-002, Mar. 2005.

[13] J. Crassidis, "Sigma-point Kalman filtering for integrated GPS and inertial navigation," *IEEE Transactions on Aerospace and Electronic Systems*, vol. 42, no. 2, pp. 750-756, Jun. 2006.

[25] G. Allibert, D. Abeywardena, M. Bangura, and R. Mahony. "Estimating body-fixed frame velocity and attitude from inertial measurements for a quadrotor vehicle." in *Proc. of the IEEE Conf. on Control Application (CCA)*, Juan Les Antibes, France, Oct. 2014, pp. 978-983.

[14] J. Crassidis and F. Markley, "Unscented Filtering for Spacecraft Attitude Estimation," *Journal of Guidance, Control, and Dynamics*, vol. 26, no. 4, pp. 536-542, 2003.

[15] K. Sebesta and N. Boizot, "A Real-Time Adaptive High-Gain EKF, Applied to a Quadcopter Inertial Navigation System," *IEEE Transactions on Industrial Electronics*, vol. 61, no, 1, pp. 495-503, Jan. 2014.

[16] S. Sarkka and A. Nummenmaa, "Recursive Noise Adaptive Kalman Filtering by Variational Bayesian Approximations," *IEEE Transactions on Automatic Control*, vol. 54, no. 3, pp. 596-600, Mar. 2009.

[17] H. Qian, W. Huang, L. Qian and C. Shen, "Robust extended Kalman filter for attitude estimation with multiplicative noises and unknown external disturbances," IET Control Theory & Applications, vol. 8, no, 15, pp. 1523-1536, Oct. 2014.

[18] A. Kumar and J. Crassidis, "Colored-Noise Kalman Filter for Vibration Mitigation of Position/Attitude Estimation Systems," in *Proc. of the AIAA Guidance, Navigation and Control Conference and Exhibit*, Hilton Head, SC, USA, Aug. 2007.

[19] R. Lozano, P. Castillo, P. Garcia and A. Dzul, "Robust prediction-based control for unstable delay systems: Application to the yaw control of a mini-helicopter," *Automatica*, vol. 40, no. 4, pp. 603-612, 2004.

[20] R. Sanz, P. Garcia, P. Castillo and P. Albertos, "Time-delay compensation using inertial measurement sensors for quadrotor control systems," in *Proc. of the 17th Intl. Conference on Information Fusion*, Salamanca, Spain, Jul. 2014, pp. 1-6.

[21] Q. Jia, "Disturbance Rejection Through Disturbance Observer With Adaptive Frequency Estimation," *IEEE Transaction on Magnetics*, vol. 45, no. 6, pp. 2675-2678, Jun. 2009.

[22] R. M. Murray, Z. Li and S. S. Sastry, *A Mathematical Introduction to Robotic Manipulation*. Boca Raton, FL, USA: CRC Press, 1994.

[23] F. Bullo and R. Murray, "Proportional derivative (pd) control on the euclidean group," in European Control Conference, vol. 2, pp. 1091-1097, 1995

[24] E.J. Lefferts, F.L. Markley, and M.D. Shuster, "Kalman Filtering for Spacecraft Attitude Estimation," *Journal of Guidance, Control, and Dynamics* vol. 5, no. 5, pp. 417-429, 1982.

[26] J. P. Hespanha, *Linear systems theory*. Princeton university Press, 2009.